NONLINEAR ANALYSIS OF RENFORCED FIBROUS CONCRETE VIERENDEEL TRUSS

Prof. Kalid Shaker Mahmod **Aalaa Whaleed Hameed**

ABSTRACT:

A Vierendeel truss is a hyper static frame composed of a series of rectangular or trapezoidal panels with out diagonal members. The end conections of all members are rigid and designed to take moment. In this work, the use of fiber reinforced concrete in construction of Vierendeel trusses with nonlinear material behavior is researched. The addition of randomly dispersed discrete steel fibers to concrete improves many engineering properties of the material such as fracture toughness, fatigue resistance, impact resistance and flexural strength. Several parameters that affected the behavior of the structure like fiber volume fraction, aspect ratio, and the position of the portion in structure that used fibrous concrete are studied. All these studies are hold out by developing a program, named (P3DNFEA).

الخلاصة:

مسنم فرنديل هو هيكل مستقر يتألف من سلسلة من الفضاءاتالمستطيلة أو المعينية المنحرفة وبدون عوارض قطرية. مناطق الاتصال لاعضاء المسنم تصمم لان تكون جاسئة وتتحمل عزوم. خلال هذا البحث, يتم استخدام الخرسانة المسلحة و المحتوية على الياف فولاذية في انشاء المسنمات الفرنديلية مع الاخذ بنظر الاعتبار التصرف الاخطي للمواد. ان اضافة الالياف الفولاذية الموزعة بشكل عشوائي في الخرسانة يحن عدد من الصفات الهندسية للمادة (الخرسانة) مثل مقاومة الكسر, مقاومة الكلل, مقاومة الصدمات و مقاومة الالتواء. العوامل التي تؤثر على تصرف المنشأ مثل نسبة تواجد الالياف, طول الليف وقطره, و الموقع من المنشأ الحاوي على خرسانة مسلحة بالالياف قد أخذت بنظر الاعتبار. كل هذه الدراسات تمت من خلال تطوير برنامج اسمه P3DNFEA.

KEYWORD

Finite element, fibrous concrete.

INTRODUCTION

The Vierendeel truss, in spite of its designation, is not a truss in the conventional sense of being an assemblage of connected triangular unit, but a rigid frame. The diagonals are omitted and the chords and web members are made fully continuous to obtain stability. In addition, Vierendeel truss: offers some esthetic qualities, has simple details because of the limited number of members at a joint, is easier to form and place, and can be pre-casted or cast in place.

Both steel and reinforced concrete have been used as material construction. Moreover, Vierendeel girders are used in structures where free unobstructed space is required between the top and bottom chords. Fig. (1) show an arc-welded steel truss of this type.

Fig. 1 Bent-Leg spandrel columns with Vierendeel bracing, Hoover Support Team.

FINITE ELEMENT

20-nodes brick elements have been used for representing concrete element, as n Fig. (2). In each twenty-nodes, three degrees of freedoms (translation) u, v and w are along the Cartesian coordinate X, Y and Z, respectively.

While for reinforcement bar the embedded representation is used. In this type of representation, the reinforcement bars are assumed as line element, which is capable of transmitting axial force only.

The idealization of fibers effect were perform in the tension-stiffening model used as a result of fiber addition. That was in (P3DNFEA) program, while in the ANSYS program the effect of fibers were introduced by concerning fibers as bar.reinfocement with small fraction.

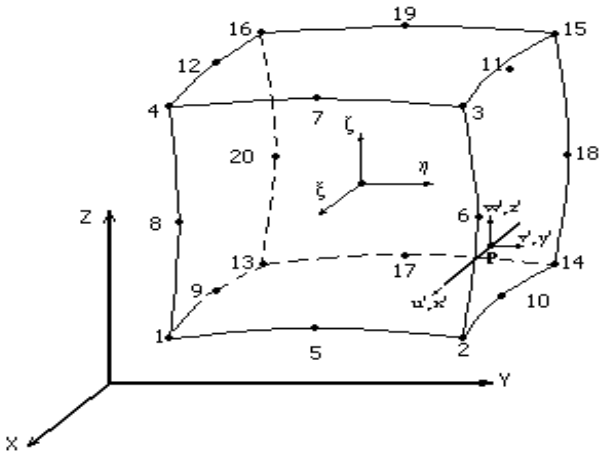

Fig. 2 20-node element in global and local coordinates with the definition of steel bar location.

Numerical Integration

One of the most accurate and convenient methods is "Gaussian quadrature", and which is used here. Gaussian quadrature is suited for numerical integration of polynomials for finite elements where dimensionless parameters (such as ζ, η and ξ) are used, and the origin is located at the center, Fig. 3.

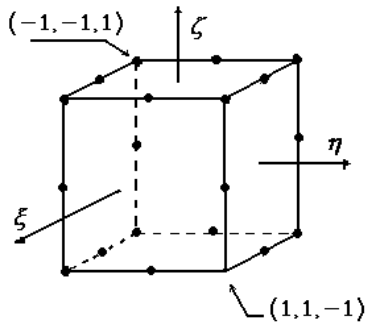

Fig. 3 Local coordinate system.

Nonlinear Solution Techniques

An incremental-iteration procedure is used through this work, Fig. 4. here, the load is applied incrementally, but after each increment successive iterations are performed.

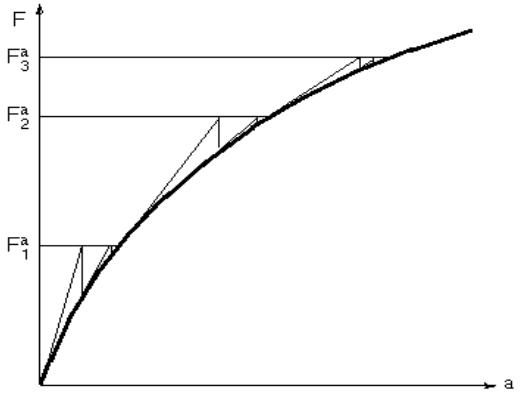

Fig. 4 The incremental-iteration procedure.

MATERIALS PROPERTIES

The main feature of plain concrete is its high compressive strength compared to its low tensile strength and low energy absorption capacity, as well, the brittleness behavior of failure mode. Therefore, to overcome these shortcomings, one may incorporate high-strength, small diameter fibers into the composites, and a new material can be gained, called fiber concrete or fibrous concrete.

Uniaxial Compression Behavior

The addition of fibers is shown to increase toughness much more than the first crack strength. In Fig. (5 and 6), which are the stress-strain curves in compression for SFR mortar (ACI committee 544), one can recognize a substantial increase in the strain at peak stress, and the slope of the decending portion is less steep than that of control specimens without fibers. This is an indication of substantially higher toughness, where toughness is a measure of ability to absorb energy during deformation.

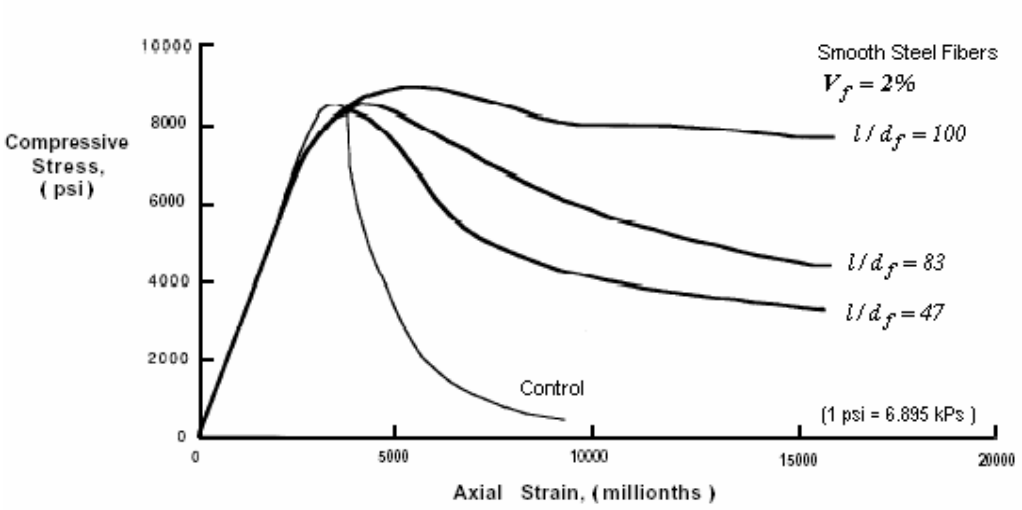

Fig. 5 Influence of the aspect ratio on the stress-strain curve, ACI committee 544.

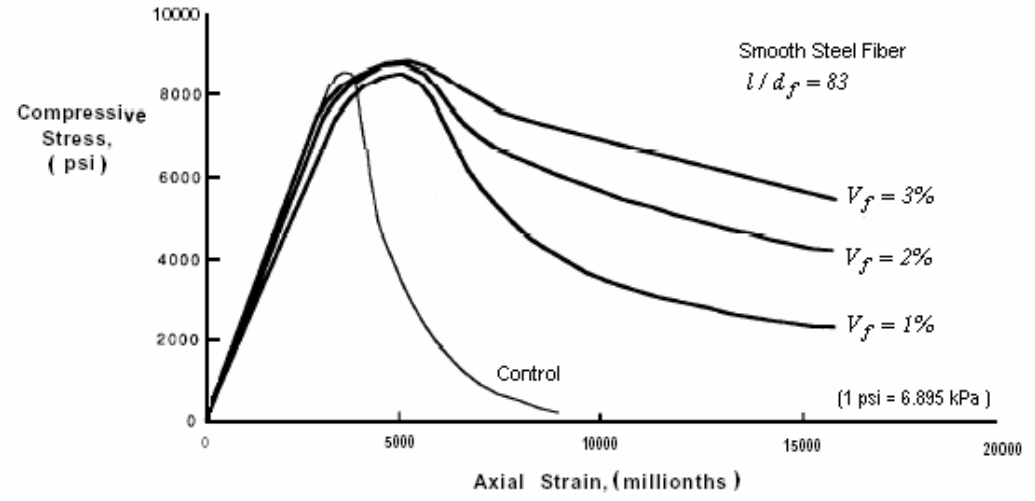

Fig. 6 Influence of te volume fraction of fibers on the compressive stress-strain curve[1].

Uniaxial Tensile Behavior

The strength mechanism of the fibers involves transfer of stress from the matrix to the fibers by interfacial shear, or by interlock between the fibers and the matrix if the fibers surfaces are deformed. Stress is, thus, shared by the fibers and the matrix in tension until the matrix crakes. Then the total stress is progressively transferred to the fibers. In tension, SFRC fails only after the steel fiber breaks or is pulled out of the cement matrix.

Multiaxial Behavior

The biaxial strength of fiber concrete is significantly greater than that of plain concrete. Fig. 7 shows a biaxial strength envelopes for plain and fiber concrete.

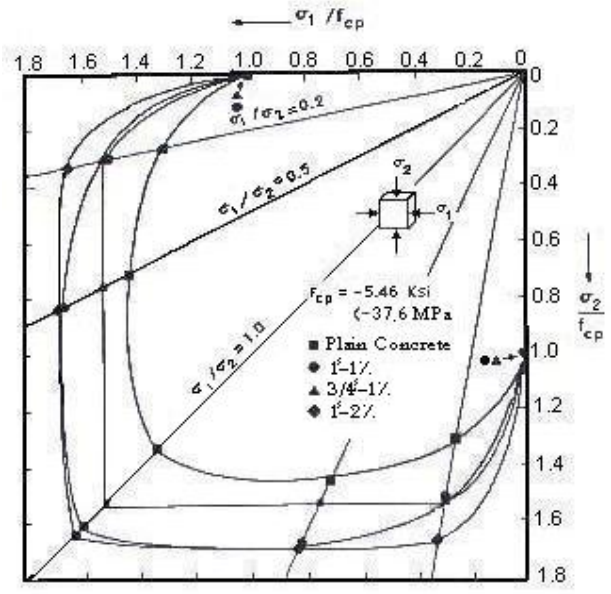

Fig. 7 Biaxial strength envelops for plain and fiber concrete[10].

The mechanical behavior of steel fiber reinforced concrete subjected to multiaxial loading may be assumed to be similar to that of plain concrete, its strength and ductility increase with the increase of confining pressure.

In this study the formulation presented by Soroushian and Lee for obtaining the stresses and strains in both compression and tension is used:

* For compression:

$$f_{cf}' = f_c' + 3.6 \times \left(V_f \cdot L_f\right)/d_f \quad (1)$$

$$\varepsilon_{pf} = 0.0021 + 0.007\left(V_f \cdot L_f\right)/d_f \quad (2)$$

* For tension:

$$f_{tf} = f_t\left(1 + 0.016N_f^{1/3} + 0.05\pi \cdot d_f \cdot L_f \cdot N_f\right) \quad (3)$$

$$\varepsilon_{tf} = \varepsilon_t\left(1 + 0.35N_f \cdot d_f \cdot L_f\right) \quad (4)$$

Where:

N_f : Number of fibers per unit cross-section area

MATERIAL MODELING

Modeling of Concrete

Behavior of Concrete in Compression

In the present study, the behavior of concrete in compression is simulated with an elastic-plastic work hardening model followed by perfect plastic response, which is terminated at the onset of crushing. The plasticity model can be illustrated in terms of the following constructions:

1. The Yield Criterion.

2. The Hardening Rule.
3. The Flow Rule.
4. The Crushing Condition.

The Yield Criterion

In the present work, a yield criterion based on two stress invariants has been adopted, and this is given by:

$$f(\sigma) = f(I_1, J_2) = \left[\alpha \cdot I_1 + 3\beta \cdot J_2\right]^{1/2} = \sigma_o \tag{5}$$

The Hardening Rule

The hardening rule defines the motion of the subsequent yield surfaces during plastic loading. A number of hardening rules has been proposed to describe the growth of subsequent yield surfaces for work-hardening materials, these are:

1. isotropic hardening rule.
2. kinematics-hardening rule.
3. mixed hardening rule.

Here, the isotropic hardening rule is adopted. The subsequent loading functions may be expressed as:

$$f(\{\sigma\}) = c \cdot I_1 + \left\{(c \cdot I_1)^2 + 3\beta \cdot J_2\right\}^{1/2} = \bar{\sigma} \tag{6}$$

The Flow Rule

So far, the loading surface alone is considered, mention has been made of the plastic stress-strain relations. The necessary connection between the loading function, ***f***, and the stress-strain relation for a work-hardening material will be made here by means of a flow rule. In plasticity theory the flue rule is defined so that the increments of plastic strain can be evaluated from a given stress state. An associated flow rule will be employed here. This means that the plastic deformation rate vector will be assumed to be normal to the adopted yield surface. The plastic strain increment is defined as:

$$d\{\varepsilon^p\} = d\lambda \cdot \frac{\partial f(\{\sigma\})}{\partial \{\sigma\}} = d\lambda \cdot \{a\} \tag{7}$$

The yield function derivatives with respect to the stress components define the flow vector as:

$$\{a\} = \left[\frac{\partial f}{\partial \sigma_x} \quad \frac{\partial f}{\partial \sigma_y} \quad \frac{\partial f}{\partial \sigma_z} \quad \frac{\partial f}{\partial \tau_{xy}} \quad \frac{\partial f}{\partial \tau_{yz}} \quad \frac{\partial f}{\partial \tau_{xz}}\right]^T \tag{8}$$

The Crushing Condition

The described hardening–plastic model governs the increase of the elastic deformation in concrete under compressive stress. Inelastic deformation continues in the concrete until crushing occurs. The crushing type of fracture is a strain-controlled phenomenon. A failure surface in the stress space must be defined so that this kind of fracture can be taken into account. Despite the lack of experimental data on concrete ultimate deformation capacity under multiaxial loading, crushing criterion is obtained by, simply, converting the yield criterion, equation 5 which is described in terms of stresses, directly into strains, thus:

$$cI_1' + \left\{(cI_1')^2 + 3\beta \cdot J_2'\right\}^{1/2} = \varepsilon_{cu} \tag{9}$$

Behavior of Concrete in Tension

Probably, the main feature of plain concrete material behavior is its low tensile strength, which results in tensile cracking at a very low stress compared with the failure stress in compression. However, the addition of steel fibers the mix will enhance the tensile strength and change the brittle failure to ductile one.

A smeared crack model will be adopted in this work. To understand and deal with such model, the following items have to be studied:

1. Cracking Criterion.
2. Tension Stiffening.
3. Shear Retention.

The Cracking Criterion

The tensile strength of uncracked concrete can be obtained from laboratory tests. Usually, concrete properties are deduced from the compressive strength. Simple criteria are, therefore, favored by most analysts to predict tensile fracture. Maximum tensile stress or maximum tensile strain criterion is, usually, used for this purpose. Here, the tensile type of fracture is the maximum tensile stress criterion (tension cut-off)[6]. For previously uncracked sampling point, the principal stresses and there directions are evaluated. if the maximum principal stress exceeds a limiting value, a crack is formed in a plane orthogonal to it. The limited tensile stress required defining the onset of cracking, which can be calculated for states of triaxial tensile stress and for combinations of tension and compression principal stresses as follows:

(a) For the triaxial tension zone $(\sigma_1 \geq \sigma_2 \geq \sigma_3 > 0)$

$$\sigma_i = \sigma_{cr} = f'_{tf} \qquad i = 1,2,3 \tag{10}$$

(b) For the tension-tension-compression zone $(\sigma_1 \geq \sigma_2 > 0, \sigma_3 \leq 0)$

$$\sigma_i = \sigma_{cr} = f'_{tf}\left[1 + \frac{0.75\sigma_3}{f'_{cf}}\right] \qquad i = 1,2 \tag{11}$$

(c) For the tension-compression-compression zone $(\sigma_1 > 0, \sigma_3 \leq \sigma_2 \leq 0)$

$$\sigma_i = \sigma_{cr} = f'_{tf} \cdot \left[1 + \frac{0.75\sigma_2}{f'_{cf}}\right] \cdot \left[1 + \frac{0.75\sigma_3}{f'_{cf}}\right] \tag{12}$$

Tension Stiffening Model

The reinforcement and the concrete are both subjected to tension, so that, large cracks are formed. The opening of cracks occurs at the same time as boned failure and relative movement between the bar and concrete takes place. The shear force at the contact surface feed tension stresses into the concrete between the crakes. The concrete hangs on the bare and contributes to over-all stiffness of the system. This stiffness effect is often called tension stiffening. The phenomenon is represented by the descending part of the stress-strain curve. The model proposed by Yin et. al.,1989, is used though this work, and it is defined as follows:

a) For $\varepsilon_{cr} \leq \varepsilon_n \leq \varepsilon_{tf1}$

$$\sigma_n = \alpha_2 \cdot \sigma_{cr} \quad (13)$$

b) For $\varepsilon_n \geq \varepsilon_{tf1}$

$$\sigma_n = 0 \quad (14)$$

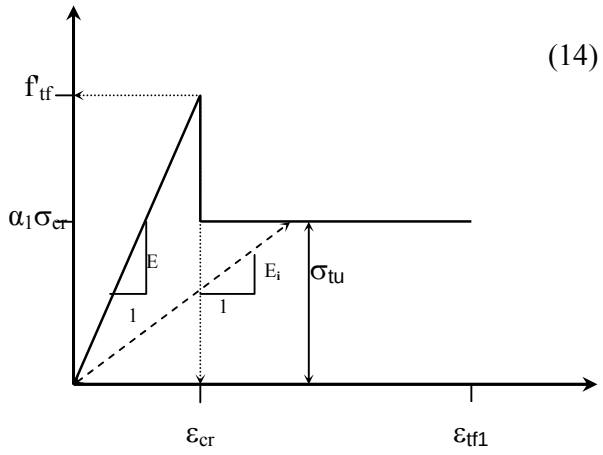

Fig. 8 Post-cracking model of steel fiber reinforced concrete.

Shear Retention Model

The shear stiffness at a cracked sampling point becomes progressively smaller as the crack widens. So the shear modulus of elasticity is reduced to βG, fig. 9. The following relations are used to account for the shear retention effect.

a) For $\varepsilon_n < \varepsilon_{cr}$

$$\beta = 1.0 \quad (15)$$

b) For $\varepsilon_{cr} < \varepsilon_n < \alpha_1.\varepsilon_{cr}$

$$\beta = \frac{\gamma_2 - \gamma_3}{\gamma_1 - 1}\left[\gamma_1 - \frac{\varepsilon_n}{\varepsilon_{cr}}\right] + \gamma_3 \quad (16)$$

c) For $\varepsilon_n > \alpha_1.\varepsilon_{cr}$

$$\beta = \gamma_3 \quad (17)$$

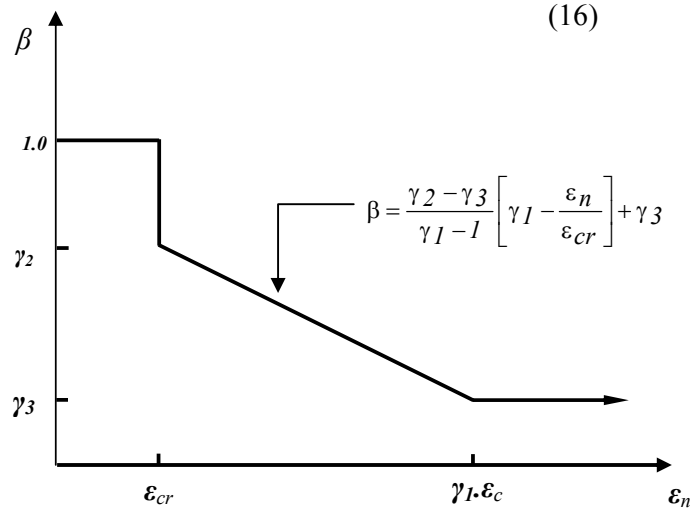

Fig. 9 Shear retention model for concrete.

Modeling of Reinforcement

Reinforcing steel is a homogenous material and has, usually, the same strength in tension and compression. In the present work, an elastic-linear work hardening model simulates the uniaxial stress-strain behavior of steel bars, as in fig 10

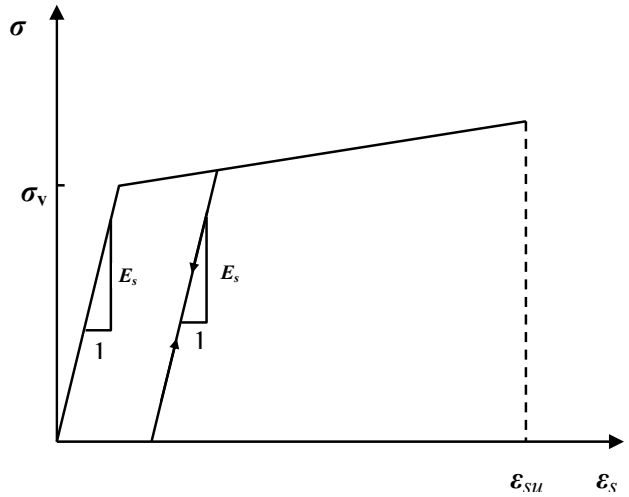

Fig.10 Stress-strain relationship of steel bars used in the analysis.

PARAMETRIC STUDY

Three Vierendeel structures are analyzed here. These structures have been tested by Alwash (1995). Each structure is subjected to a mid-span concentrated load applied at the upper chored. The details of geometry and arrangement of reinforcements for these structures are shown in figs. (11-a, b, c)

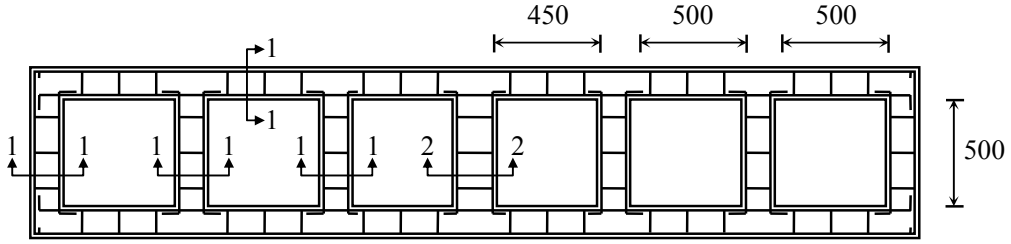

Fig. 11-a Geometry and arrangement of reinforcements for VER1.

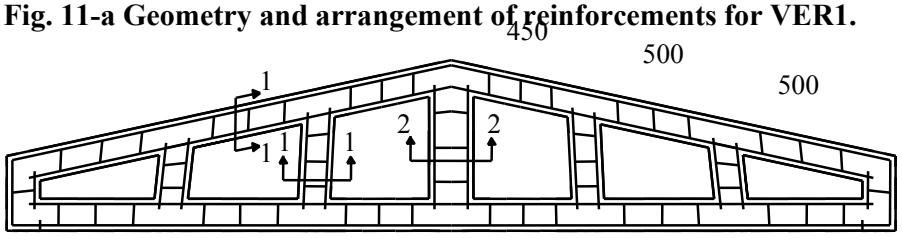

Fig. 11-b Geometry and arrangement of reinforcements for VER2.

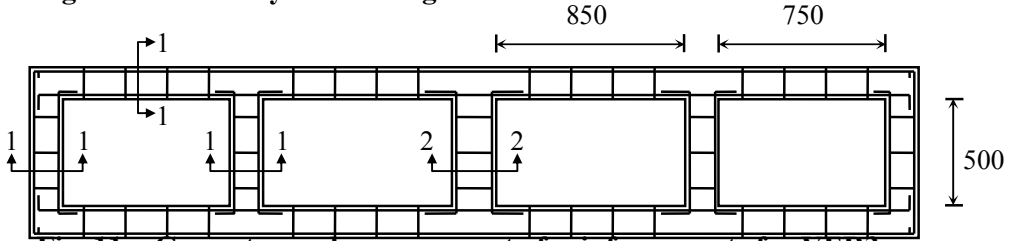

Fig. 11-c Geometry and arrangement of reinforcements for VER3.

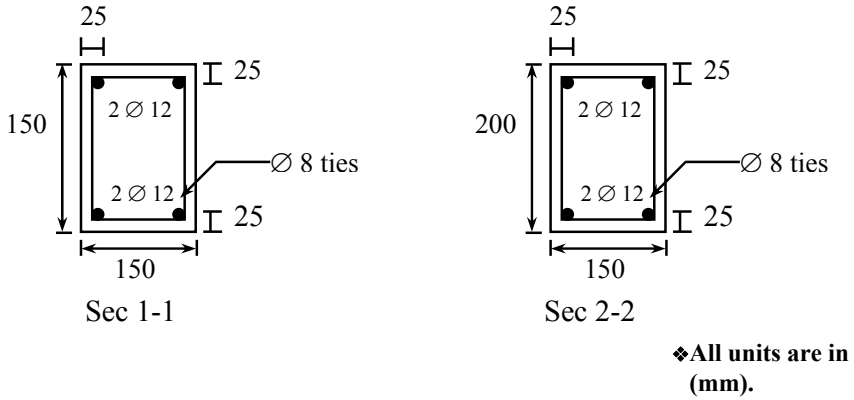

Fig. 11 Details of geometry and arrangement of reinforcements.

Structure shape

From thes three different shapesof Vierendeel trusses, two comparison cases are provided, one for voids number and size, and the other for the inclination of top chord.

Voids number and size

This comparison is carried out between VER1 and VER3. VER1 has six voids; their size varies from (500*500 mm) to (450*500 mm). On the other side, VER3 has four voids; their size varies from (750*500 mm) to (850*500 mm) here and after referring to Fig. 12, one can conclude that: when the number of voids is lessened on the expense of the increase in the voids size leads to a remarkable decrease (by 17.8%) in the structure rigidity and increase in the average deflection (by 14.1%).

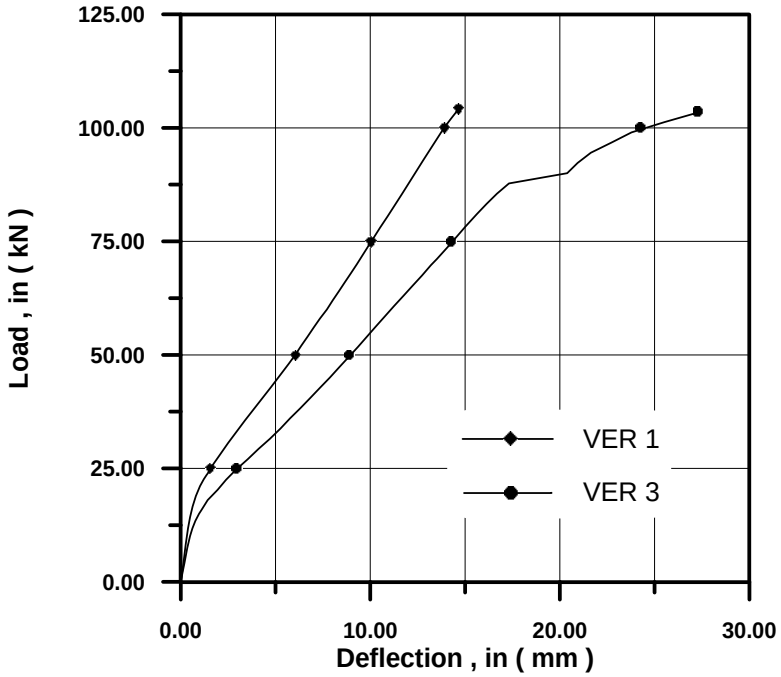

Fig. 12 Influence of voids number and size.

Inclination of top chord

By increasing the inclination of top chords from (inclination=0) to (inclination =12.4^{o}) structure strength increase with decreasing in its deflection, by (10.57%) and (36.71%), respectively, as in Fig. 13.

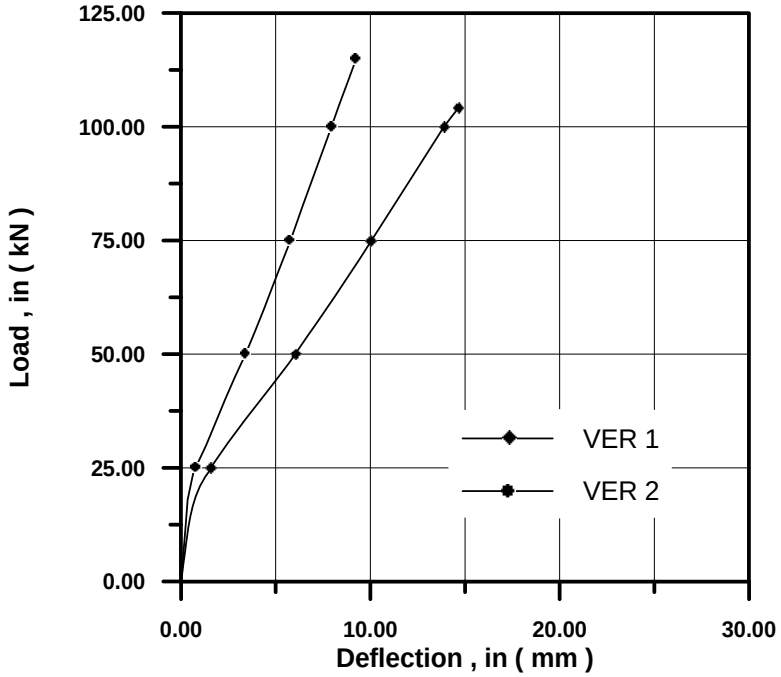

Fig. 13 Influence of inclination of top chord.

Fibers distribution

Three cases are searched to examine the influence of fibers distribution position through the structure. In the *first* case, fibers are distributed through the whole structure. While in the *second* case, fibers are distributed just in the bottom boom where the tensile stress is expected to be high. Finally, in the *third* case, fibers are distributed in both bottom boom (where expected high tensile stress) and vertical members (where the shear stress expected to be high and influential). The comparisons between these three cases are clearly shown in Figs. (14, 15, 16).

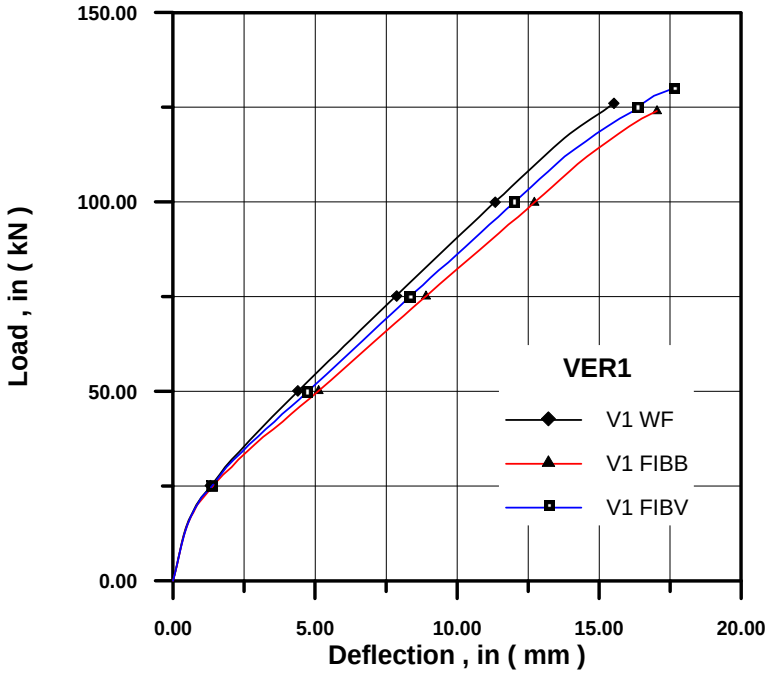

Fig. 14 The influence of fibers distribution in VER1.

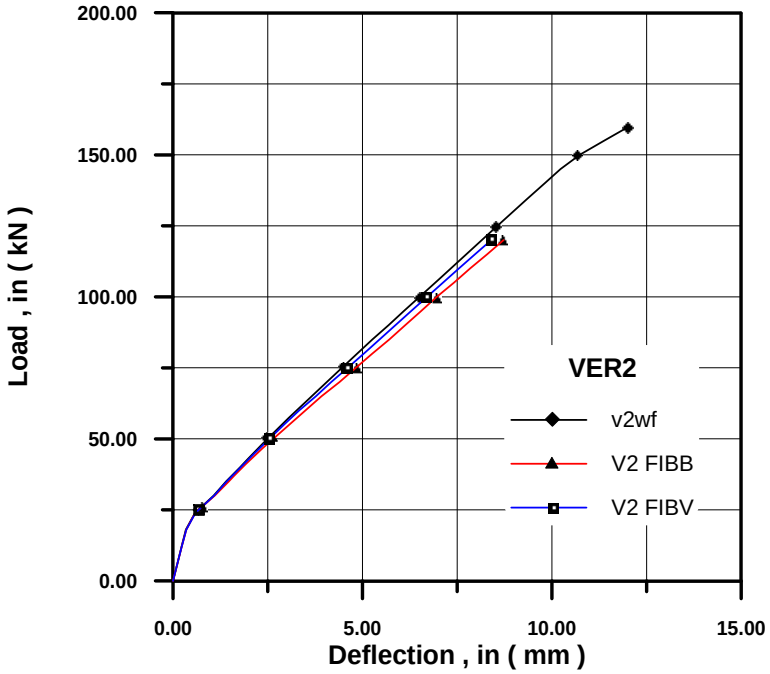

Fig. 15 The influence of fibers distribution in VER2.

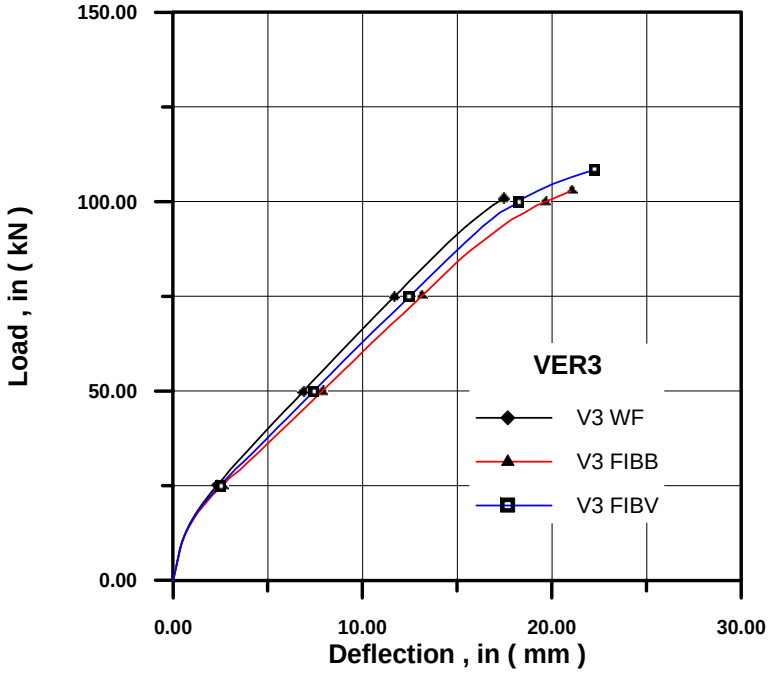

Fig. 16 The influence of fibers distribution in VER3.

When fiber geometries are changed like fiber length fiber diameter or fiber volume fraction, it seen to be affecting the response of structure which will be explained through the following notes:

1. When increasing V_f , a substantial increasing in structure rigidity is noticed, as in Fig 17. This is because of increasing in the crack arrestors. Therefore, delaying structure failure.

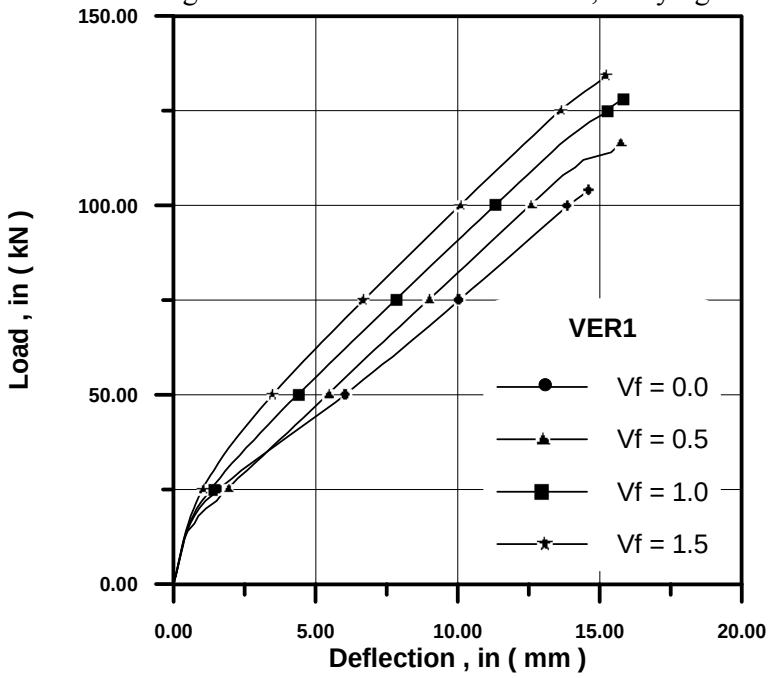

Fig. 17 Effect of V_f .

2. The matrix contains fibers distributed through it fail by two way. Either by fiber pull-out (this happened when fiber is short) or by fiber yield (this happened when fiber is long). The needed stress for the former type of failure is much more than the latter one. Therefore, when increasing L_f , an increasing in structure rigidity is observed.

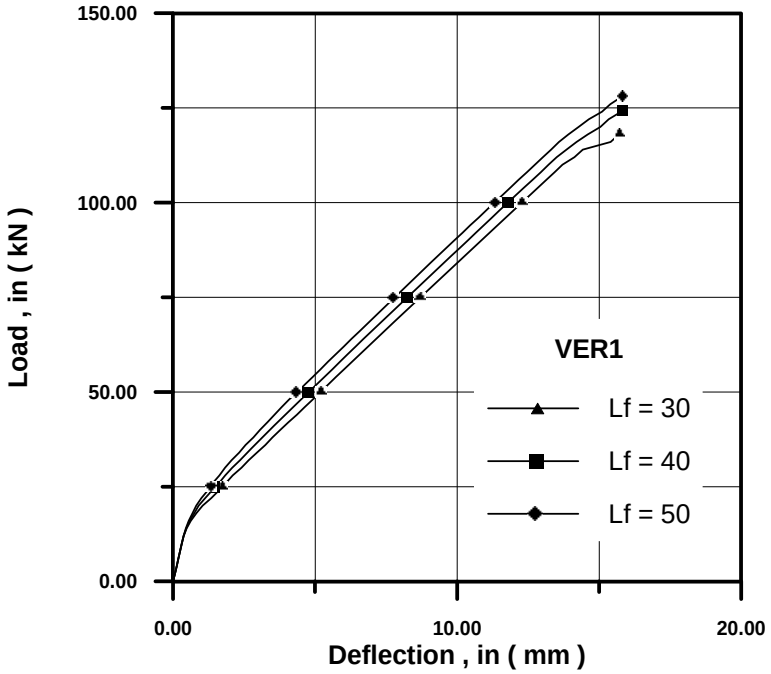

Fig. 18 Effect of L_f.

3. Here, the effect of d_f show a differ behavior than V_f and L_f, i.e., when increasing V_f, structure rigidity decreases.

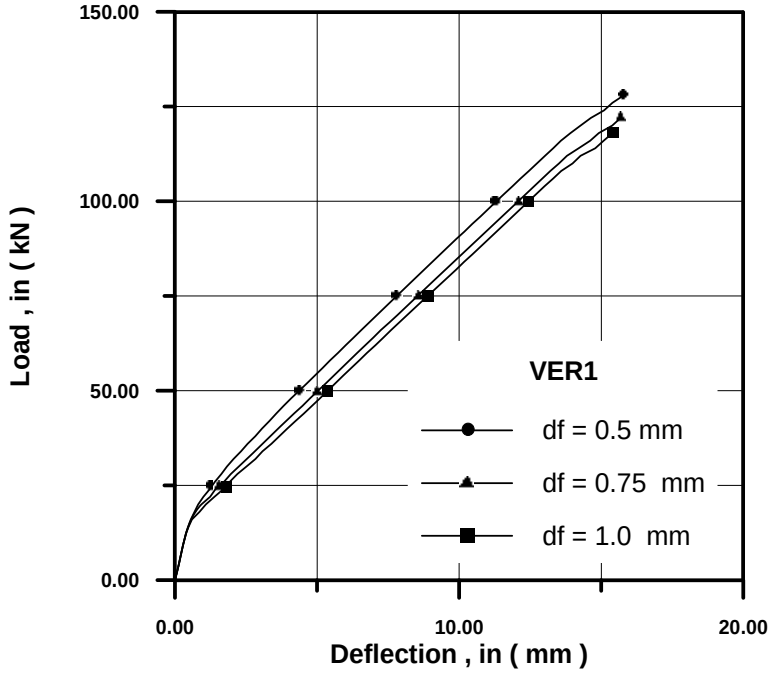

Fig. 19 Effect of d_f.

STRESSES STUDY

Here the stress distribution in Y-direction, with a sketch for the crack propagation through different load stages can be viewed. One can depend on this survey to decide on and through which portion fibers are to be distributed.

Stress distribution propagate in concrete

In Fig. 20 stress distribution in Y-direction for VER1 at mid-span

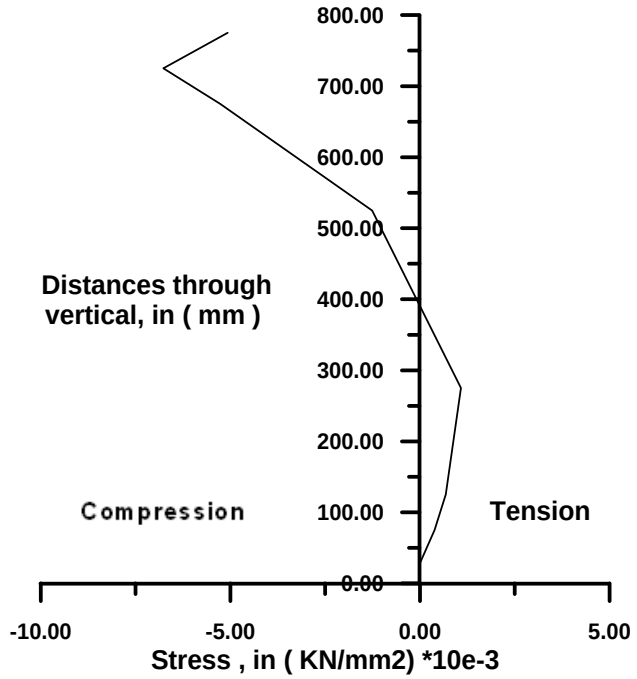

Fig. 20 Stress distribution in Y-direction for VER1 at mid-span.

Fig. 21 Stress distribution in Y-direction for VER1, (N/mm^2).

Here and from Figs. 20 and 21, both distributions have similarity for half of the structure. The compressive and tensile zones are appearing clearly in these figures. By considering that the barrier between the compressive and tensile zones is a shear zone, the shear appears in the middle of verticals and near joints; while the tensile zone is more dominating in bottom booms.

Stress distribution through the longitudinal main bars

Fig. 22 shows the stress distribution and development for the bottom steel bars.

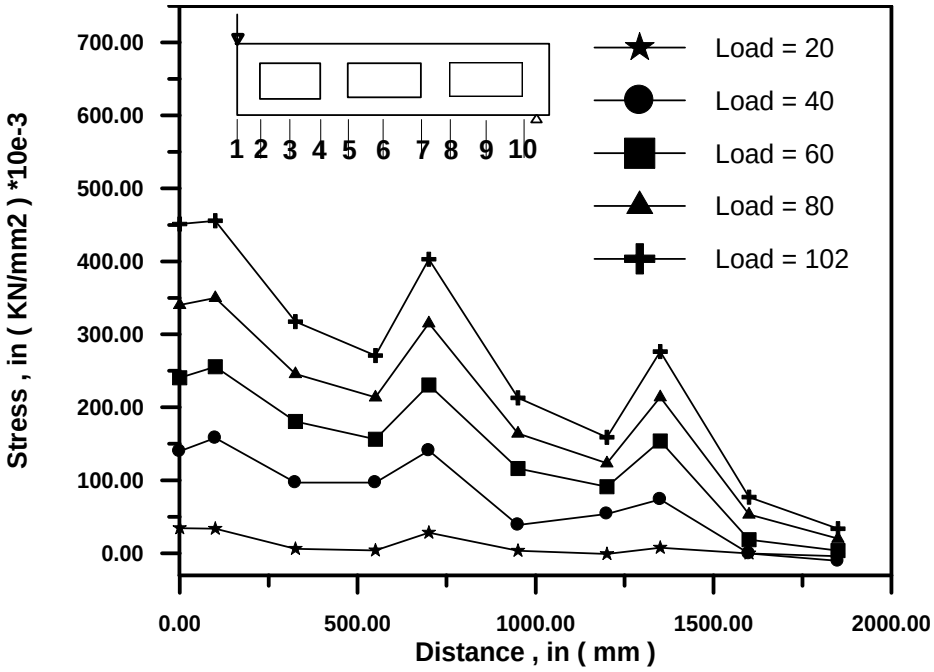

Fig 22 Stress distribution and development for the bottom steel bars of VER1.

This longitudinal stress reaches its maximum magnitude at mid-span, where maximum number of cracks exists, and decreases gradually as close from support, with some inflection points appear through structure holes. By increasing the applied load, the stress distribution magnitude increases indicating that the steel bars carry the stress release from the cracked concrete to achieve the equilibrium.

Crack pattern

Figs. (23-a, b, c and d) show the crack distribution and propagation through different load stages

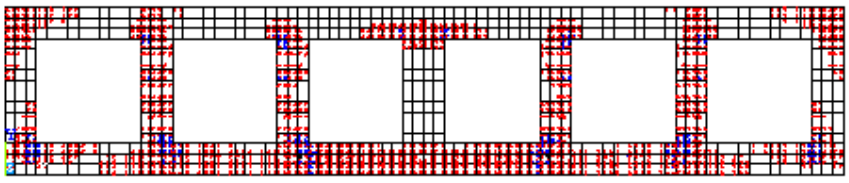

Fig. 23-a Crack pattern of VER1 at load (45 kN).

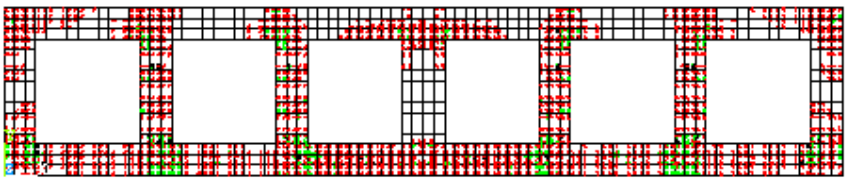

Fig. 23-b Crack pattern of VER1 at load (60 kN).

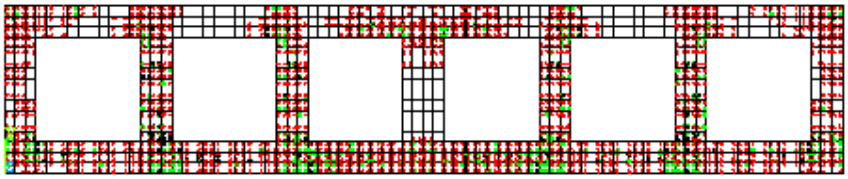

Fig. 23-c Crack pattern of VER1 at load (75 kN).

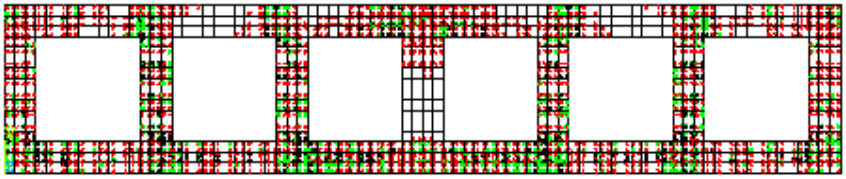

Fig. 23-d Crack pattern of VER1 at load (90 kN).

CONCLUSIONS

* The developed program has shown good agreement with experimental data of (Taan and Swamy) and ANSYS program in case of fibrous concrete.
* The use of inclined chords is recommended, because this inclination greatly reduces the bending stress.
* The use of steel fiber increases strength by (16.93 %) while deflection is decreased by (15.335 %) for the examples considered herein.
* The use of steel fibers is shown to increase the toughness much more than the first crack strength.
* The addition of steel fibers enhances the tensile strength, crack resistance, crack control.
* Fiber length, fiber diameter and fiber volume fraction influence the mechanical properties of steel fiber reinforced concrete.
* The usage of steel fibers may particularize in the tension and shear zones only for economical purposes.
* Tension zone is concentrated in central bottom chords with some fragmentary portions in structure, while shear zone is concentrated in verticals and middle of outer chords.
* Stress in steel bars has some inflection points because of change in stress distribution.

REFRENCES

- Al-Sha'arbaf (1990), "Three-Dimensional Nonlinear Finite Element Analysis of Reinforced Concrete Beams in Torsion" Ph.D. Thesis, University of Bradford, 1990.
- Alwash, N. A. K., "Nonlinear Finite Element Analysis of Reinforced Vierendeel Trusses", Ph.D. Thesis, University of Technology, 1995.

- Cervera, M., Hinton, E. and Hassan, O., "Nonlinear Analysis of Reinforced Concrete Plat and Shell Structures Using 20-Noded Isoparametric Brick Elements", computer and structure, Vol.25, No.6, p.p. (845-869), 1987.
- Chandrupatla and Belegundu, " Introduction to Finite Elements in Engineering", Prentice-Hall International, Inc.
- Chen, W.F., "Plasticity in Reinforced Concrete", McGraw-Hill Book company.
- Hannant, D. J., " Fiber Cement and Fiber Concrete", JOHN WILEY & SONS.
- Hoover Support Team, www.hoverdambypass.org, PDF file
- Jenn-Chuan Chern, et. al, "Behavior of Steel Fiber Reinforced Concrete in Multiaxial Loading" ACI materials journal, Vol. 89, No.1, January-February 1992, p.p. (32-40).
- Manual of concrete practice 1985, ACI committee 544, part5.
- Soroushain, P., and Lee, C. D., "Constitutive Modeling of Steel Fiber Reinforced Concrete under Direct Tension and Compression" Proceeding of the Inter. Conf. on the Recent Developments In Fiber Reinforced Cements And Concrete, 18-20 September 1989, Cardiff (U. K.), Eds. Swamy and Barr, p.p. (363-377).
- Traina, L. A., and Mansour, S. A., "Biaxial Strength And Deformational Behavior Of Plain And Steel Fiber Concrete" ACI material journal, Vol.88, No.4, July-Augost 1991, p.p. (354-362).
- Yin, W.S., et al, "Biaxial Tests of Plain and Fiber Concrete" ACI materials journal, Vol.86, No.3, May-June 1989, p.p. (236-243).
- Young D., "Analysis of Vierendeel Truss" ASCE transportation paper No. 1973, p.p (869-938).

NOTATIONS

$\{a\}$	Flow vector
d_f	Fiber diameter
$f(\sigma)$	Yield surface, yield function
f'_{cf}	Compressive strength of fiber reinforced concrete
f_{tf}	Tensile strength of fiber reinforced concrete
I_1	first invariant of the stress tensor
and J_2 J_3	second and third invariant of the deviator stress tensor
L_f	Fiber length
N_f	Number of fibers per unit cross-section area
V_f	Volume fraction of fiber

α_1	Rate of strain decay
α_2	Sudden loss in stress ration
β	Shear reduction factor
ε	Strain
ε_{cf}	The total strain
ε_{cu}	Ultimate strain value that can be extrapolated from the ultimate compressive test
ε_{tf}	Tensile strain of fiber reinforced concrete
γ_1	Rate of decay of shear stiffness as the crack widens
γ_2	Ratio of sudden loss in shear at the instant of cracking
γ_3	Ratio of the residual shear stiffness due to the dowel
$d\lambda$	A factor determining the size of the plastic strain increment
σ	Stress
σ_o	Equivalent effective stress at onset of plastic deformation
$\bar{\sigma}$	Effective stress or the equivalent uniaxial stress
σ_{cr}	Cracking stress
τ_u	Shear stress between the fiber and the concrete
ξ , η and ζ	Local coordinate